OXFORD

Human Molecular Genetics, 2015, Vol. 24, No. 13 3699–3707

doi: 10.1093/hmg/ddv114
Advance Access Publication Date: 8 April 2015
Original Article

ORIGINAL ARTICLE

Vitreal delivery of AAV vectored Cnga3 restores cone function in *CNGA3*$^{-/-}$/*Nrl*$^{-/-}$ mice, an all-cone model of CNGA3 achromatopsia†

Wei Du[1], Ye Tao[1], Wen-Tao Deng[1], Ping Zhu[1], Jie Li[1], Xufeng Dai[1,2], Yuxin Zhang[1,3], Wei Shi[1], Xuan Liu[1], Vince A. Chiodo[1], Xi-Qin Ding[4], Chen Zhao[3], Stylianos Michalakis[5], Martin Biel[5], Zuoming Zhang[6,*], Jia Qu[2,*], William W. Hauswirth[1,*] and Ji-jing Pang[1,2,3,*]

[1]Deparment of Ophthalmology, University of Florida, Gainesville, FL 32610, USA, [2]School of Ophthalmology and Optometry, The Eye Hospital, Wenzhou Medical University, Wenzhou, Zhejiang 325027, China, [3]Department of Ophthalmology, The First Affiliated Hospital of Nanjing Medical University and State Key Laboratory of Reproductive Medicine, Nanjing Medical University, Nanjing 210029, China, [4]Department of Cell Biology, University of Oklahoma Health Sciences Center, Oklahoma City, OK 73104, USA, [5]Munich Center for Integrated Protein Science and Department of Pharmacy, Center for Drug Research, Ludwig-Maximilians-Universität München, 81377 Munich, Germany and [6]Department of Clinical Aerospace Medicine, Fourth Military Medical University, Xi'an 710032, China

*To whom correspondence should be addressed at: Department of Ophthalmology, College of Medicine, University of Florida, 1600 SW Archer Road, Gainesville, FL 32610, USA. Tel: +1 3522739341; Fax: +1 3523920573; Email: jpang@ufl.edu

Abstract

The *CNGA3*$^{-/-}$/*Nrl*$^{-/-}$ mouse is a cone-dominant model with *Cnga3* channel deficiency, which partially mimics the all cone foveal structure of human achromatopsia 2 with CNGA3 mutations. Although subretinal (SR) AAV vector administration can transfect retinal cells efficiently, the injection-induced retinal detachment can cause retinal damage, particularly when SR vector bleb includes the fovea. We therefore explored whether cone function–structure could be rescued in *CNGA3*$^{-/-}$/*Nrl*$^{-/-}$ mice by intravitreal (IVit) delivery of tyrosine to phenylalanine (Y-F) capsid mutant AAV8. We find that AAV-mediated CNGA3 expression can restore cone function and rescue structure following IVit delivery of AAV8 (Y447, 733F) vector. Rescue was assessed by restoration of the cone-mediated electroretinogram (ERG), optomotor responses, and cone opsin immunohistochemistry. Demonstration of gene therapy in a cone-dominant mouse model by IVit delivery provides a potential alternative vector delivery mode for safely transducing foveal cones in achromatopsia patients and in other human retinal diseases affecting foveal function.

† The authors wish it to be known that, in their opinion, the first two authors should be regarded as joint First Authors.

Received: February 4, 2015. **Revised:** March 16, 2015. **Accepted:** March 30, 2015

Introduction

The human retina has ~6 million cone photoreceptors and 100 million rod photoreceptors. Cones are primarily responsible for central high resolution and color vision while operating in moderate-to-bright light. They are primarily concentrated in the macula with the central foveola being nearly 100% cones. Achromatopsia, or rod monochromatism, is a recessive genetic condition characterized by cone dysfunction, with an incidence of ~1/30 000 in western populations (1). Achromats exhibit total color vision loss, poor central vision, visual acuity of 20/200 or worse (2) and daylight blindness (photosensitivity), making them legally blind. Clinically, the first signs of achromatopsia in infants are nystagmus and photosensitivity as evidenced by squinting in bright light (2). Both rods and cones rely on cyclic nucleotide-gated (CNG) channels for photoreceptor plasma membrane hyperpolarization and signal transduction. Cone CNG channels consist of two CNGB3 subunits and two CNGA3 subunits. In European populations, ~25% of patients with achromatopsia have *CNGA3* mutations, ~50% have *CNGB3* mutations, and smaller fractions have mutations in the cone transducin or phosphodiesterase genes (3). Moreover, in the Middle East (4) and China (5), the fraction of achromatopsia due to *CNGA3* mutations is likely significantly >25%.

Recent progress in adeno-associated viral (AAV)-based gene replacement therapy to restore cone-mediated function and visual behavior in *CNGA3* deficient mouse models provides a foundation for the development of clinical trials for human achromatopsia patients (6–8). In these studies, AAV vectors containing Cnga3 cDNA were delivered subretinally in *CNGA3*$^{-/-}$ or *cpfl5* mice, which carry a naturally occurring mutation in the *Cnga3* gene.

The challenge for achromatopsia gene therapy and the desirability to develop an intravitreal (IVit) injection option is based on recently published results of 15 patients from the current NEI-sponsored LCA2 clinical trial (NCT00481546). Single or multiple subretinal (SR) AAV vector injections resulting in vector blebs in paramacular and more peripheral retinal areas uniformly led to robust quantitative improvements in light sensitivity, visual acuity, pupillary light response and mobility performance (9–11). In contrast, vector blebs that detached the fovea resulted in little or no vision gain for the patient and in some cases caused a slight loss in visual acuity (11). It was concluded that SR injection of vector under the fovea may cause more damage than benefit and should be approached with care, if at all. Therefore, developing alternative ways of transducing foveal cones more safely is the focus of this study. To that end, we aimed to test the IVit route of vector injection and employed novel AAV variants that we have developed in an effort to validate and optimize the ability to correct cone defects in mouse models of achromatopsia without detaching the retina.

The application of AAV vectors in retinal gene therapy in clinical and basic research and its limitations and strategies to optimize have been extensively reviewed recently (12). Although IVit injection of vector can transduce a large area of the inner retina without causing retinal detachment, conventional vectors in the vitreous cannot penetrate the inner retina and transduce rod or cone cells in the outer retina because of the physical barrier at the inner-limiting membrane (ILM) (13). However, successful treatments by IVit delivery have been demonstrated in degenerative retinas where AAV showed enhanced transduction capability for outer retina (14–16). Recently, it was reported that epidermal growth factor receptor protein tyrosine kinase (EGFR-PTK)-mediated tyrosine phosphorylation of exposed residues on the AAV capsid promotes ubiquitination and subsequent proteasomal degradation of AAV particles, thus limiting AAV vector transduction efficiency (17–19). Site-directed tyrosine to phenylanine (Y-F) mutagenesis of selected tyrosine residues on the AAV2 capsid surface was shown to protect vector particles from this proteasomal degradation and significantly increase AAV2 vector transduction efficiency relative to wild-type AAV2. Moreover, vectors with capsid mutations display a strong and widespread transgene expression in many retinal cells after either SR or IVit delivery (17,18,20,21). Additional studies showed that AAV8 has higher inherent photoreceptor transduction efficiency than AAV2 or 5 (17,22,23). Accordingly, using AAV8 (Y733F)-smCBA-PDE6b (smCBA is a shortened version of the widely used CBA promoter), we obtained a more robust and longer-term rescue than with wild-type AAV8 or AAV5 vectors in the rd10 mouse, an early onset photoreceptor degenerative mouse model (24). Recently, we found that many cones could be transduced following IVit injection of AAV8 (Y447, 733F), driven by a cone-specific promoter that targets all cone cell types in normal C57 BL/6J mice (J. Pang, unpublished data).

In this study, we test whether the AAV8 (Y447, 733F) capsid can penetrate the inner retina and rescue cone function in *CNGA3*$^{-/-}$/*Nrl*$^{-/-}$ mice after IVit injection. The *CNGA3*$^{-/-}$/*Nrl*$^{-/-}$ mouse serves as a unique mammalian cone-dominant model with a CNGA3 channel deficiency. This double knock-out mouse model possesses genetically and phenotypically well-characterized cone degeneration (25) and partially mimics the foveal structure–function of human achromatopsia 2 with CNGA3 mutations, i.e. impaired cone function and cone degeneration, hence serving as a useful model to explore cone gene therapy for human achromatopsia. CNGA3$^{-/-}$/Nrl$^{-/-}$ mice lack cone-mediated ERG response, and rod-mediated scotopic light response due to its Nrl deficiency. Expression levels of M-opsin, S-opsin, Gnat2, and arrestin4 were all reduced in *CNGA3*$^{-/-}$/*Nrl*$^{-/-}$ mice. Furthermore, cone photoreceptors start to degenerate as early as postnatal Day 15 (P15), similar to single *CNGA3* knock-out mice (26). Therefore, this model permits testing of the retina-penetrating properties of AAV8 (Y447, 733F) from the vitreous for functional and structural cone rescue with reference.

Results

AAV8 (Y447, 733F) vector restores cone-mediated ERGs in *CNGA3*$^{-/-}$/*Nrl*$^{-/-}$ mice following either SR or IVit injection

Photopic ERGs at stimulus intensity of 1.4 log cd-s/m^2 were restored at 2 months and were maintained for at least 6 months following either IVit or SR injection of AAV8 (Y447, 733F)-IRBP/GNAT2-mCNGA3 to *CNGA3*$^{-/-}$*Nrl*$^{-/-}$ eyes (sample ERG traces are shown in Fig. 1A). The photopic b-wave ERG amplitudes for all animals tested are shown in Figure 1B. Following IVit injection, amplitudes ranged from 5.1 to 206.5 μV at 2 months and 42.5–103.5 μV at 6 months after treatment. These values are somewhat lower than recorded for SR vector which ranged from 100 to 290.1 μV at 2 months and 110–150 μV at 6 months.

To confirm experimentally that IVit-AAV8-(Y447, 733F) vector was accurately delivered to the vitreous and was not delivered accidentally to the SR space, we mixed cone-specific therapeutic AAV8 (Y447, 733F)-IRBP/GNAT2-mCNGA3 vector with an AAV2 (Y444, 500, 730F)-smCBA-GFP vector that transduces distinct populations of retinal cells depending on whether it is delivered to the vitreous or SR space (20). One mouse had one eye subretinally injected and the other eye intravitreally injected with this vector mixture. Photopic ERG rescue was seen in both eyes at 2 months post-injection. These ERG b-wave responses are circled in

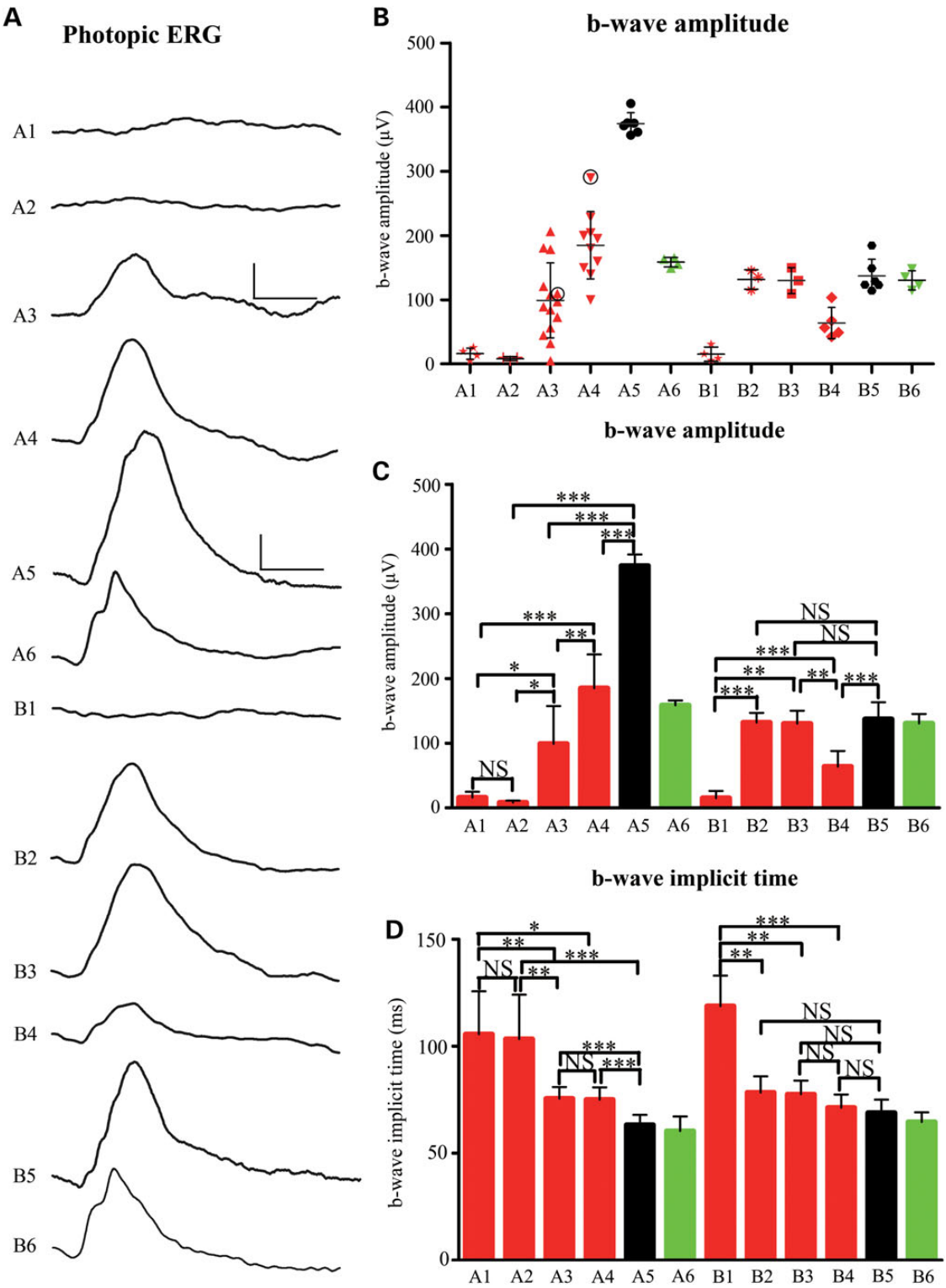

Figure 1. Photopic electroretinograms (ERGs) and statistical analysis. (**A**) Representative photopic ERG tracings elicited at 1.4 log cd-s/m^2 from *CNGA3*$^{-/-}$/*Nrl*$^{-/-}$ and control eyes. (**B**) Distribution of photopic b-wave amplitudes from each treated and untreated eyes elicited at 1.4 log cd-s/m^2 (mouse eyes which had one eye subretinally injected and the other eye intravitreally injected with a mixture of AAV8 (Y447, 733F)-IRBP/GNAT2-mCNGA3 and AAV2 (Y444, 500, 730F)-smCBA-GFP vectors are marked with circles). (**C**) Statistical analysis of photopic b-wave amplitudes elicited at 1.4 log cd-s/m^2; (**D**) Statistical analysis of photopic b-wave implicit times at 1.4 log cd-s/m^2. All of photopic ERG scale bars are the same (*y*-axis: 50 μV/Div, *x*-axis: 50 ms/Div) except for *NRL*$^{-/-}$mice at 2 months of age (*y*-axis: 100 μV/Div, *x*-axis: 50 ms/Div). NS, no statistical difference; *$P < 0.05$; **$P < 0.001$; ***$P < 0.0001$. A1 = 2.5-month-old *CNGA3*$^{-/-}$/*Nrl*$^{-/-}$ untreated eyes, A2 = *CNGA3*$^{-/-}$/*Nrl*$^{-/-}$ eyes 2 months after AAV5 IVit injection at P14, A3 = *CNGA3*$^{-/-}$/*Nrl*$^{-/-}$ eyes 2 months after AAV8 (Y447, 733F) IVit injection at P14, A4 = *CNGA3*$^{-/-}$/*Nrl*$^{-/-}$ eyes 2 months after AAV8 (Y447, 733F) SR injection at P14, A5 = 2.5-month-old NRL$^{-/-}$ eyes, A6 = 2.5-month-old C57 BL/6J eyes, B1–B6 groups are similar as those of A1–A6, but the time is 6/6.5 months instead of 2/2.5 months.

Figure 1B, and these two retinas used for immunohistochemistry (Fig. 3C) immediately after the ERG recording. The tracer GFP in IVit-treated eyes showed inner retinal GFP expression (Fig. 3C) typical for vitreal vector (20). In contrast, tracer GFP in SR-treated eyes showed photoreceptor and RPE GFP signal typical for SR vector. Therefore, both IVit and SR vector injections were anatomically accurate.

AAV5 vector did not restore cone-mediated ERG in *CNGA3*$^{-/-}$/*Nrl*$^{-/-}$ mice 2 months following IVit injection with photopic ERG responses almost undetectable (8.33 ± 2.89 μV, $n = 3$). Photopic b-wave ERG amplitudes for IVit-AAV8 (Y447, 733F) were significantly larger (98.96 ± 58.43, $n = 14$, $P = 0.02$) than that of untreated eyes (16.05 ± 8.861, $n = 4$, $P = 0.01$), being ~28% of that of the age-matched *Nrl*$^{-/-}$ controls (356.9 ± 35.15 μV, $n = 5$) and 55% of that of SR AAV8 (Y447, 733F)-treated eyes (179.8 ± 58.19 μV, $n = 10$). B-wave kinetics were also significantly improved in IVit-AAV8 (Y447, 733F)-treated eyes (75.56 ± 5.37 ms, $n = 8$) compared with that of untreated eyes (105.6 ± 20.06 ms, $n = 4$, $P = 0.002$), but were somewhat delayed compared with age-matched *Nrl*$^{-/-}$ mice (63.21 ± 4.78 ms, $n = 7$). IVit AAV5-treated *CNGA3*$^{-/-}$/*Nrl*$^{-/-}$ eyes exhibited no improvement in implicit times over untreated controls (103.3 ± 20.82 ms, $n = 3$, Fig. 1D).

To measure the persistence of functional rescue, cone-mediated ERGs were also performed at 6 months following IVit-AAV8 (Y447, 733F) treatment. The average photopic b-wave amplitudes (Fig. 1C) were 63.76 ± 24.05 μV ($n = 3$) and 15.20 ± 11.03 μV ($n = 4$) in treated and untreated *CNGA3*$^{-/-}$*Nrl*$^{-/-}$ eyes, respectively. Treated eyes had ~46% of the b-wave amplitude of control age-matched *Nrl*$^{-/-}$ eyes (137.2 ± 25.94 μV $n = 6$). Significant differences remained between photopic b-wave amplitudes of IVit-AAV8 (Y447, 733F) treated and untreated *CNGA3*$^{-/-}$*Nrl*$^{-/-}$ eyes ($P = 0.0006$), and between IVit-AAV8 (Y447, 733F) treated *CNGA3*$^{-/-}$*Nrl*$^{-/-}$ eyes and age-matched *Nrl*$^{-/-}$ eyes ($P = 0.0009$). Compared with 118.8 ± 14.29 ms for b-wave implicit times in untreated CNGA3$^{-/-}$/Nrl$^{-/-}$ eyes, IVit-AAV8 (Y447, 733F) treated eyes were significantly improved (71.25 ± 6.185 ms) and statistically similar to age-matched *Nrl*$^{-/-}$ control eyes (68.88 ± 6.169 ms, $n = 4$, $P = 0.6062$) (Fig. 1C).

AAV8 (Y447, 733F), but not AAV5-mediated CNGA3 expression restores optomotor responses in *CNGA3*$^{-/-}$/*Nrl*$^{-/-}$ mice following vitreal vector treatment

We then test whether restoration of cone ERG function translated into improvement in cone-mediated visual behavior by measuring optomotor responses to rotating sine-wave gratings (27). Under photopic conditions, untreated *CNGA3*$^{-/-}$/*Nrl*$^{-/-}$ eyes performed poorly (Fig. 2A). Consistent with ERG responses, optomotor performance improved only after IVit-AAV8 (Y447, 733F), not after IVit-AAV5 at 2 months post-treatment (Fig. 2). For IVit AAV5-treated eyes, visual acuities (0.077 ± 0.016 cyc/deg, $n = 4$, Fig. 2A) and contrast sensitivities (1.066 ± 0.032, Fig. 2B) were nearly identical to those of the untreated *CNGA3*$^{-/-}$/*Nrl*$^{-/-}$ eyes (visual acuity: 0.057 ± 0.017 cyc/deg; contrast sensitivity: 1.037 ± 0.021, $n = 4$, $P = 0.1198$ and 0.1404, respectively). In contrast, IVit-AAV8 (Y447, 733F) treated eyes showed an average visual acuity of 0.447 ± 0.032 cyc/deg. ($n = 4$, Fig. 2A) and a contrast sensitivity of 8.205 ± 0.442 (Fig. 2B), significantly better than those from untreated *CNGA3*$^{-/-}$/*Nrl*$^{-/-}$eyes ($P < 0.0001$), but not as good as those from age-matched *Nrl*$^{-/-}$ eyes (visual acuity: 0.510 ± 0.018 cyc/deg; contrast sensitivity: 9.473 ± 0.599; $P = 0.0016$ and 0.0019, respectively). At 6 months following injection, IVit-AAV8 (Y447, 733F)-treated eyes showed an average visual acuity of 0.346 ± 0.041 cyc/deg ($n = 3$, Fig. 2A) and contrast sensitivity of 7.176 ± 1.470 (Fig. 2B), significantly better than those of untreated *CNGA3*$^{-/-}$/*Nrl*$^{-/-}$eyes ($P < 0.0001$), but again less than those from age-matched *Nrl*$^{-/-}$ eyes (visual acuity: 0.437 ± 0.045 cyc/deg; contrast sensitivity: 8.589 ± 0.250; $P = 0.0414$ and 0.0016, respectively). In all cases, SR treatment with either vector yielded significantly improved visual acuity and contrast sensitivity, as expected (Fig. 2).

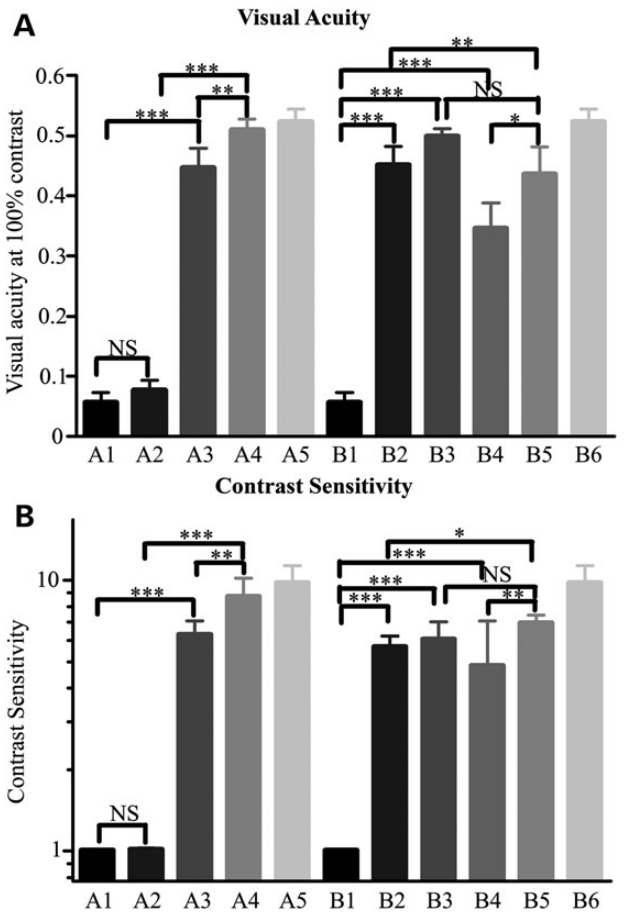

Figure 2. Intravitreal delivery of AAV8 (Y447, 733)-IRBP/GNAT2-mCNGA3 restores photopic visual acuity and contrast sensitivity in *CNGA3*$^{-/-}$/*Nrl*$^{-/-}$ mice. (**A**) Comparison of average values for photopic acuities. (**B**) Comparison of average values for photopic contrast sensitivities; NS, no statistical difference, *$P < 0.05$, **$P < 0.001$, ***$P < 0.0001$. Labels are same as those in Figure 1. A1 = 2.5-month-old *CNGA3*$^{-/-}$/*Nrl*$^{-/-}$ untreated eyes, A2 = *CNGA3*$^{-/-}$/*Nrl*$^{-/-}$ eyes 2 months after AAV5 IVit injection at P14, A3 = *CNGA3*$^{-/-}$/*Nrl*$^{-/-}$ eyes 2 months after AAV8 (Y447, 733F) IVit injection at P14, A4 = 2.5-month-old NRL$^{-/-}$ eyes, A5 = 2.5-month-old C57 BL/6J eyes; B1 = 2.5-month-old *CNGA3*$^{-/-}$/*Nrl*$^{-/-}$ untreated eyes, B2 = *CNGA3*$^{-/-}$/*Nrl*$^{-/-}$ eyes 2 months after AAV5 IVit injection at P14, B3 = *CNGA3*$^{-/-}$/*Nrl*$^{-/-}$ eyes 2 months after AAV8 (Y447, 733F) IVit injection at P14, B4 = *CNGA3*$^{-/-}$/*Nrl*$^{-/-}$ eyes 2 months after AAV8 (Y447, 733F) SR injection at P14, B5 = 2.5-month-old NRL$^{-/-}$ eyes, A6 = 2.5-month-old C57 BL/6J eyes.

AAV8 (Y447, 733F), but not AAV5-mediated CNGA3 expression was detected in cones following IVit injection

Six months after SR or IVit vector treatment, CNGA3 expression was assayed by immunohistochemistry (Fig. 3). Age-matched wild-type C57BL/6J mice showed robust outer segment (OS) CNGA3 expression (Fig. 3A). CNGA3 expression was also detected in CNGA3$^{-/-}$/Nrl$^{-/-}$ eyes following SR-AAV5 or IVit-AAV8 (Y447, 733F) treatment, whereas the contralateral uninjected eyes lacked

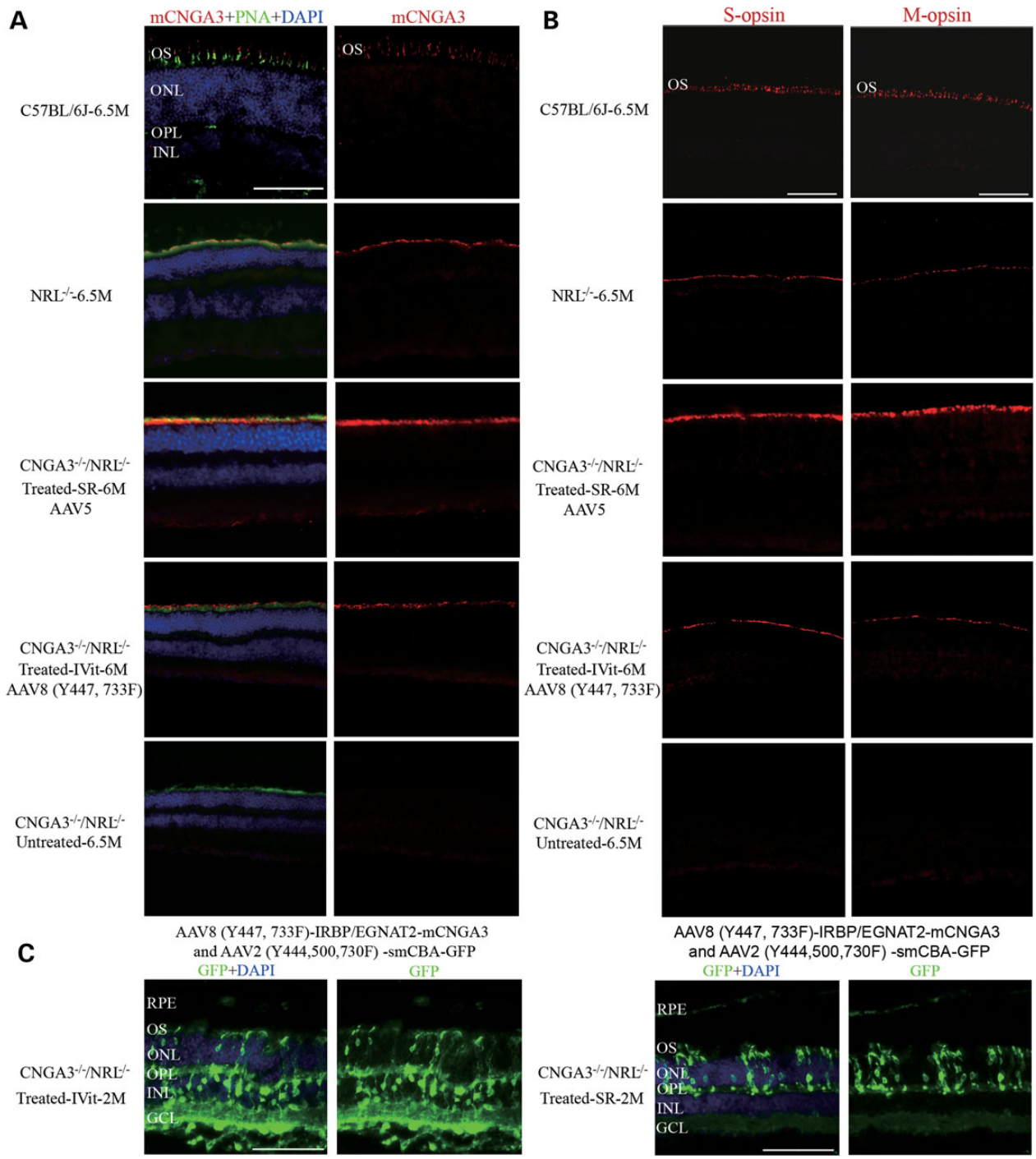

Figure 3. IVit-AAV8 (Y447, 733)-mediated mCNGA3 expression leads to cone opsin preservation in treated $CNGA3^{-/-}/Nrl^{-/-}$ eyes. (**A**) Six months post-IVit injection, frozen retinal sections immunostained with anti-mouse CNGA3 antibody and cone-specific PNA showing mouse CNGA3 expression in OSs of age-matched control C57 BL/6J and $Nrl^{-/-}$ eyes, SR-AAV5 and IVit-AAV8 (Y447, 733) treated eyes, but not in untreated $CNGA3^{-/-}/Nrl^{-/-}$ eye. (**B**) Frozen retinal sections immunostained with S- or M-opsin antibody from the same eyes as in (A) showing S- or M-opsin expression in OSs of C57 BL/6J, $Nrl^{-/-}$, SR AAV5 and IVit-AAV8 (Y447, 733) treated eyes; little S- or M-opsin staining was detected in contralateral untreated $CNGA3^{-/-}/Nrl^{-/-}$ eye. (**C**) Frozen retinal section from one $CNGA3^{-/-}/Nrl^{-/-}$ mouse immunostained with GFP antibody 2 months after treatment with a mixture of AAV8 (Y447, 733)-IRBP/GNAT2-mCNGA3 and AAV2 (Y444, 500, 730F)-smCBA-GFP (ERG responses of these two eyes marked with circles in Fig. 1B). Left panel: intravitreally injected eye, with GFP signal primarily in cells of the inner retina and photoreceptors. Right panel: subretinally injected eye with GFP expressed primarily in photoreceptors and RPE cells. RPE, retinal pigment epithelium; OS, outer segment layer; ONL, outer nuclear layer; OPL, outer plexiform layer; INL, inner nuclear layer; GCL, ganglion cell layer. Red, CNGA3, S- or M-opsin staining as indicated; green, GFP (green fluorescence protein); blue, DAPI (4′,6-diamidino-2-phenylindole dihydrochloride) stained nuclei; PNA, lectin peanut agglutinin. Scale bar = 100 μm.

detectible CNGA3 labeling. Co-localization of mouse CNGA3 and cone-specific lectin peanut agglutinin (PNA) (Fig. 3A) confirmed that CNGA3 expression was localized to cone OSs.

Because $CNGA3^{-/-}/Nrl^{-/-}$ mice exhibit a progressive loss of cone photoreceptors, most opsins are absent at 7 months of age (25). As for $Nrl^{-/-}$ mice, cone OSs of $CNGA3^{-/-}/Nrl^{-/-}$ mice are

never well developed and very short around this age (Fig. 3). Cone opsins in *CNGA3*$^{-/-}$/*Nrl*$^{-/-}$ mice were maintained 6 months after P14 SR injection of either AAV8 (Y447, 733) or AAV5 vector with therapeutic gene (Fig. 3B). The positive M- and S-opsin staining reported here confirms that cone degeneration was prevented by IVit-AAV8 (Y447, 733) treatment (Fig. 3B). Furthermore, the accuracy of our vitreal injections is additionally confirmed because in no case did IVit AAV5 vector lead to functional or structural rescue, whereas SR AAV5 yielded measurable rescue by all functional and structural parameters (see above).

Discussion

CNG channels play a central role in phototransduction. Mutations in the cone CNG channel subunits CNGA3 and CNGB3 account for >70% of all known cases of achromatopsia (28,29). CNGA3$^{-/-}$ mice undergo a progressive loss of cone photoreceptors, with cones in the ventral retina nearly absent by 3 months of age (26). A subsequent study showed that CNGA3$^{-/-}$/Nrl$^{-/-}$ mice had a retinal phenotype similar to the sum of their respective single knock-out counterparts, i.e. impaired cone function and cone degeneration (25). Cone OS in Nrl$^{-/-}$ retinas are shorter than wild type, with occasional abnormalities of the outer nuclear layer at an early age, referred to as rosettes (30,31). *Nrl*$^{-/-}$ cones undergo a slow degeneration so that by 31 weeks of age many cone opsin-positive cells have degenerated and nearly all rosettes have disappeared (32). Although only 28% of the age-matched Nrl$^{-/-}$ photopic ERG amplitudes were restored in *CNGA3*$^{-/-}$/ Nrl$^{-/-}$ eyes at 2 months following IVit-AAV8 (Y447, 733F) treatment, this fraction increased to 46% by 6 months. One reason for this is that cone ERGs at 6 months are at <2 months in Nrl$^{-/-}$ mice due to the loss of cone rosettes and the slow cone loss as noted above. Since IVit vector must transit the inner retina before reaching cones, vector titer is reduced before reaching their intended cone target, and this likely accounts for the less-than-complete rescue of cone function by IVit vector.

To distinguish between whether IVit-AAV8 (Y447, 733F) vectors were reaching cones through inner retinal layers as intended or through some vector being delivered inadvertently to the SR space, AAV8 (Y447,733)-IRBP/GNAT2-mCNGA3 vector and a nontherapeutic AAV2 (Y444, 500, 730F)-smCBA-GFP tracing vector, which have distinct transfection patterns whether delivered intravitreally or subretinally, were injected together into CNGA3$^{-/-}$/Nrl$^{-/-}$ eyes. Intravitreally delivered vector mixture clearly had a GFP expression pattern diagnostic for vitreal vector while the other eye, with the mixture subretinally injected, had a GFP expression pattern expected of SR vector. Critically, following injection at either site resulted in cone ERG rescue, and, as expected, both now exhibited positive CNGA3 expression in cones (data not shown). This confirms that vitreal AAV8 (Y447, 733) vector can indeed penetrate inner retinal layers before reaching cones and mediate a therapeutic response in CNGA3$^{-/-}$ cones.

The restoration of cone-mediated retinal function observed in IVit-AAV8 (Y447, 733)-IRBP/GNAT2-mCNGA3 treated eyes was also supported by behavioral responses collected by optokinetic testing. AAV5 vector, quite therapeutic subretinally, restores neither visual acuity nor contrast sensitivity following IVit treatment in *CNGA3*$^{-/-}$/*Nrl*$^{-/-}$ mice (Fig. 2), further confirming the accuracy of our IVit vector delivery.

Validation here of the retina-penetrating property of AAV8 (Y447, 733F) by the IVit injection route in CNGA3$^{-/-}$/Nrl$^{-/-}$mice has implications for current human gene therapy paradigms, where damage caused by SR delivery is a concern (9–11). However, there are potentially critical differences between mouse and human retinal anatomies that may be relevant. First, the ILM that separates the vitreous from the retina is much thicker in primates than in rodents (33); hence, the barrier for a penetrating vector may be higher in primates. Second, rodents have no macula or fovea and have fully intact inner retinal layers spanning the central retina, whereas in the primate fovea the inner retinal cells have been displaced concentrically outward during development (34), leaving few inner retinal cells for a vitreal vector to transit before contacting foveal cones. Moreover, the thick primate ILM outside the central fovea thins considerably over the central fovea (33). This likely accounts for reports of foveal cone transduction by even unmodified vitreal AAV vectors but no transduction of more peripheral photoreceptors (35). In short, these data suggest that if central foveal cones are the retinal disease target, AAV vectors may be quite useful. As such, the vector technology reported here could be potentially very useful in treating foveal cones in a variety of cone maladies, including multiple genetic forms of achromatopsia, in which both foveal and extrafoveal cones would be therapeutic targets, and other cone dystrophies such as blue cone monochromatism, red-green color blindness, early macular degeneration or late stage retinitis pigmentosa. In addition, mutagenesis of surface exposed threonine (T) residues to valine (V) or alanine (A) may also increase transduction efficiency by decreasing phosphorylation of capsid and subsequent ubiquitination as part of the proteosomal degradation pathway (18,36,37). Retina-penetrating AAV variants, like the AAV8 (Y447,733F) vector studied here or the other similar novel AAV vectors (38), may also have application for gene delivery to retinal pigmented epithelial (RPE) cells located behind the fovea and for more peripheral rods and cones as well. This would greatly expand the therapeutic usefulness of retinal gene therapy. Full validation of whether this new class of AAV vectors has application to human retinal disease will now require its careful evaluation in nonhuman primates.

In summary, using an intravitreally delivered AAV8 (Y447,733)-IRBP/GNAT2-mCNGA3 vector, we have shown for the first time that gene therapy effectively restores cone function in a mouse without the potentially retina damaging effects of SR vector delivery. Our results suggest that intravitreally delivered AAV-mediated gene replacement therapy has the potential to become a safer therapeutic option than currently possible for human achromatopsia and other cone maladies.

Materials and Methods

Animals

C57 BL/6J mice were obtained from the Jackson Laboratory (Bar Harbor, ME, USA); the CNGA3$^{-/-}$ (39), Nrl$^{-/-}$ (31) (kindly provided by Dr Anand Swaroop at NEI/NIH), and CNGA3$^{-/-}$/Nrl$^{-/-}$(25) mice were generated as described previously. Eighty mice with both sexes from ages of 2 weeks to 6.5 months were used in this study with non-blind designation. All mice were maintained in the University of Florida Health Science Center Animal Care Service Facilities on a 12 h/12 h light–dark cycle with <15 cd-s/m^2 environmental illumination. All animals were maintained under standard laboratory conditions (18–23°C, 40–65% humidity) with food and water available *ad libitum*. All experiments were approved by the Institutional Animal Care and Use Committee at the University of Florida and conducted in accordance with the ARVO Statement for the Use of Animals in Ophthalmic and Vision Research and National Institutes of Health regulations.

Construction of AAV vectors

Mouse *Cnga3* cDNA (8) was cloned under the cone-specific IRBP/GNAT2 promoter (40) to make AAV-IRBP/GNAT2-mCNGA3 construct. The construct was packaged into serotypes 5 and 8 (Y447, 733F), which was originally made in Boye's lab (38). AAV2 (Y444, 500, 730F)-smCBA-GFP vector was also packaged as previously described (20). Vectors were purified and tittered according to previously published methods (41).

Subretinal and intravitreal injections

Prior to injection, each mouse was given 1% atropine eye drops to dilate the pupil starting 1 day before and the injecting day starting 5 h before anesthetization by ketamine (75 mg/kg)/xylazine (4 mg/kg) intramuscular injection. Administration of 2.5% phenylephrine hydrochloride eye drops for quick mydriasis was used every hour starting from 4 h before the anesthesia. At P14, 1 μl of AAV5-IRBP/GNAT2-mCNGA3 or AAV8 (Y447, 733F)-IRBP/GNAT2-mCNGA3 vector (both at a titer of 1×10^{13} vector genomes/ml) was injected subretinally or intravitreally into one eye of each CNGA3$^{-/-}$/Nrl$^{-/-}$ mouse. The other eye remained uninjected as a control. SR injections were performed as previously described (24,42), and only eyes with no apparent surgical complications and >80% of retinal detachment were retained for further evaluation. Trans-cornea IVit injections were performed (43). This approach avoids the possibility of vitreal vector reaching the SR space through the injection hole as may happen following trans-sclera IVit injection.

For injection of mixtures of two vectors, one microliter of an AAV8 (Y447, 733F)-IRBP/GNAT2-mCNGA3 and AAV2 (Y444,500, 730F)-smCBA-GFP mixture (both at titer of 2×10^{13} vector genome/ml) was intravitreally or subretinally injected into both the right and left eyes of five CNGA3$^{-/-}$/Nrl$^{-/-}$ mice at P14. Following the injection, one drop of 1% atropine (Hi-Tech Pharmacal Co. Inc., Amityville, NY, USA) and a small amount of Ophthalmic Ointment with Neomycin, Polymyxin B Sulfates & Dexamethasone (E. Fougera and Co., Melville, NY, USA) were applied to the eye to reduce injection-related inflammation and prevent possible infection (24,42).

Electroretinography

Electroretinogram (ERG) was performed every 2 months following SR or IVit injections. A UTAS Visual Diagnostic System with a Big Shot Ganzfeld (LKC Technologies, Gaithersburg, MD, USA) was employed using methods previously described with minor modifications (7,24,44). Age-matched C57 BL/6J and Nrl$^{-/-}$ mice were used as controls. Briefly, all mice were dark-adapted overnight and 1% atropine eye drops were given 1 h before anesthetization by ketamine (75 mg/kg)/xylazine (4 mg/kg) intramuscular injection, followed by topical administration of 2.5% phenylephrine hydrochloride eye drops. Dark-adapted ERGs were assessed at a stimulus intensity of 0.4 log cd-s/m^2 and inter-stimulus intervals of 30 s, with 10 recordings averaged. Then mice were light adapted for 10 min at an intensity of 30 cd-s/m^2 before photopic ERG measurements were recorded at stimulus intensity of 1.4 log cd-s/m^2 in the presence of continuous 30 Ganzfeld cd-s/m^2 background light with inter-stimulus intervals of 0.4 s. Fifty recordings were averaged for each light-adapted ERGs measurement. B-wave amplitudes were defined as the difference between the trough and peak of each waveform. Scotopic and photopic b-wave amplitudes were averaged and used to generate average responses and standard deviations (SD). ERG data are presented as mean ± SD. Statistical analysis was performed with unpaired *t*-test and significance defined as a *P*-value of <0.05.

Optokinetic testing

Photopic visual acuities and contrast sensitivities of treated and untreated eyes of CNGA3$^{-/-}$/Nrl$^{-/-}$ mice were measured using a two-alternative forced choice paradigm as described previously with minor modifications (24,27,42,45). Thresholds for each eye were determined simultaneously via stepwise functions for correct responses in both the clockwise and counter-clockwise directions. Acuity was defined as the highest spatial frequency (100% contrast) yielding a threshold response, and contrast sensitivity was defined as 100 divided by the lowest percent contrast yielding a threshold response (sinusoidal pattern at 0.256 cyc/deg). For acuity measurement, the initial stimulus was a 0.200 cyc/deg sinusoidal pattern with a fixed 100% contrast. For contrast sensitivity measurements, the initial pattern was presented at 100% contrast, with a fixed spatial frequency of 0.128 cyc/deg. All patterns were presented at a speed of 12 °/s. Photopic vision was measured at a mean luminance of 70 cd-s/m^2. Visual acuities and contrast sensitivities were measured for both eyes of each mouse four to six times over a period of 1–2 weeks. Treated CNGA3$^{-/-}$/Nrl$^{-/-}$ mice following either SR or IVit injection ($n = 4$), together with the age-matched Nrl$^{-/-}$ mice ($n = 4$) as reference responses, were used. Unpaired *t*-tests were carried out on acuity and contrast measurements to determine significance, defined as a *P*-value of <0.05.

Tissue preparation and immunohistochemistry

Eyes were enucleated at 2 or 6 months after injection. Retinal sections were prepared according to previously described methods (24,46). Briefly, immediately following sacrifice, the eyes were enucleated and fixed in 4% paraformaldehyde overnight at 4°C. The cornea and lens were then removed from eyes without disturbing the retinas to prepare the eyecups, which were rinsed with PBS and then cryoprotected by placing them in 30% sucrose/PBS for 4 h at 4°C. Eyecups were then embedded in cryostat compound (Tissue TEK OCT, Sakura Finetek USA, Inc., Torrance, CA, USA) and frozen at −80°C. Retinal cryosections were cut at 12 μm thickness, then rinsed in PBS and blocked in 2% normal goat serum, 0.3% Triton X-100 in 1% BSA in PBS for 1 h at room temperature. Lectin PNA conjugated to a Alexa Fluor 488 (1 : 200, L21409, Invitrogen), S-cone opsin, M-cone opsin primary antibodies (1 : 400, Millipore, Temecula, CA, USA) or rabbit polyclonal CNGA3 antibody (1 : 200) (26) was diluted in 0.1% Triton X-100 and 1% BSA in PBS, and incubated with sections overnight at 4°C. The sections were then washed three times with PBS, and incubated with IgG secondary antibody tagged with Alexa-594 (Molecular Probes, Eugene, OR, USA) diluted 1 : 500 in PBS at room temperature for 1 h and washed with PBS. Sections were mounted with Vectashield Mounting Medium for Fluorescence (H-1400, Vector Labs, Inc., Burlingame, CA, USA) and cover slipped. Sections were analyzed with a Zeiss CD25 microscope fitted with Axiovision Rel. 4.6 software. All fluorescent images were acquired using identical exposure settings.

Acknowledgements

We thank Dr Anand Swaroop for providing the Nrl$^{-/-}$ mouse line.

Conflict of Interest Statement: W.W.H. and the University of Florida have a financial interest in the use of AAV therapies, and own equity in a company (AGTC Inc.) that might, in the future, commercialize some aspects of this work.

Funding

This work was supported by National Institutes of Health Grants (EY023543 and EY018331 to J.P., EY021721 and EY022023 to W.H., and R01EY019490 to X.Q.D.), the National Natural Science Foundation of China (81371060 and 81260155 to J.P.), the Jiangsu Province Foundation for Research Innovative Team (C.Z. and J.P.), University of Florida Faculty Enhancement Opportunity Award (J.P.), Foundation Fighting Blindness Individual Investigator Award (S.B.), Macular Vision Research Foundation, Overstreet Endowment (W.H.), Research to Prevent Blindness, Inc.. National Key Basic Research Program of China (2013CB967500 to C.Z.), National Natural Science Foundation of China (81222009 to C.Z.) and the Deutsche Forschungsgemeinschaft (DFG, MB and SM).

References

1. Kohl, S., Baumann, B., Rosenberg, T., Kellner, U., Lorenz, B., Vadala, M., Jacobson, S.G. and Wissinger, B. (2002) Mutations in the cone photoreceptor G-protein alpha-subunit gene GNAT2 in patients with achromatopsia. *Am. J. Hum. Genet.*, **71**, 422–425.
2. Kohl, S., Varsanyi, B., Antunes, G.A., Baumann, B., Hoyng, C. B., Jagle, H., Rosenberg, T., Kellner, U., Lorenz, B., Salati, R. *et al.* (2005) CNGB3 mutations account for 50% of all cases with autosomal recessive achromatopsia. *Eur. J. Hum. Genet.*, **13**, 302–308.
3. Kaupp, U.B. and Seifert, R. (2002) Cyclic nucleotide-gated ion channels. *Physiol. Rev.*, **82**, 769–824.
4. Zelinger, L., Greenberg, A., Kohl, S., Banin, E. and Sharon, D. (2010) An ancient autosomal haplotype bearing a rare achromatopsia-causing founder mutation is shared among Arab Muslims and Oriental Jews. *Hum. Genet.*, **128**, 261–267.
5. Dai, X.F. and Pang, J.J. (2012) [Progress on study of achromatopsia and targeted gene therapy]. *Zhonghua Yan Ke Za Zhi*, **48**, 755–758.
6. Michalakis, S., Muhlfriedel, R., Tanimoto, N., Krishnamoorthy, V., Koch, S., Fischer, M.D., Becirovic, E., Bai, L., Huber, G., Beck, S.C. *et al.* (2010) Restoration of Cone Vision in the CNGA3(-/-) Mouse Model of Congenital Complete Lack of Cone Photoreceptor Function. *Mol. Ther.*, **18**, 2057–2063.
7. Pang, J., Boye, S.E., Lei, B., Boye, S.L., Everhart, D., Ryals, R., Umino, Y., Rohrer, B., Alexander, J., Li, J. *et al.* (2010) Self-complementary AAV-mediated gene therapy restores cone function and prevents cone degeneration in two models of Rpe65 deficiency. *Gene Ther.*, **17**, 815–826.
8. Pang, J.J., Deng, W.T., Dai, X., Lei, B., Everhart, D., Umino, Y., Li, J., Zhang, K., Mao, S., Boye, S.L. *et al.* (2012) AAV-mediated cone rescue in a naturally occurring mouse model of CNGA3-achromatopsia. *PLoS ONE*, **7**, e35250.
9. Cideciyan, A.V., Aleman, T.S., Boye, S.L., Schwartz, S.B., Kaushal, S., Roman, A.J., Pang, J.J., Sumaroka, A., Windsor, E. A., Wilson, J.M. *et al.* (2008) Human gene therapy for RPE65 isomerase deficiency activates the retinoid cycle of vision but with slow rod kinetics. *Proc. Natl. Acad. Sci. USA*, **105**, 15112–15117.
10. Cideciyan, A.V., Hauswirth, W.W., Aleman, T.S., Kaushal, S., Schwartz, S.B., Boye, S.L., Windsor, E.A., Conlon, T.J., Sumaroka, A., Pang, J.J. *et al.* (2009) Human RPE65 gene therapy for Leber congenital amaurosis: persistence of early visual improvements and safety at 1 year. *Hum. Gene Ther.*, **20**, 999–1004.
11. Jacobson, S.G., Cideciyan, A.V., Ratnakaram, R., Heon, E., Schwartz, S.B., Roman, A.J., Peden, M.C., Aleman, T.S., Boye, S.L., Sumaroka, A. *et al.* (2012) Gene therapy for leber congenital amaurosis caused by RPE65 mutations: safety and efficacy in 15 children and adults followed up to 3 years. *Arch. Ophthalmol.*, **130**, 9–24.
12. Schon, C., Biel, M. and Michalakis, S. (2015) Retinal gene delivery by adeno-associated virus (AAV) vectors: Strategies and applications. *Eur. J. Pharm. Biopharm.*, doi.org/10.1016/j.ejpb.2015.01.009.
13. Trapani, I., Puppo, A. and Auricchio, A. (2014) Vector platforms for gene therapy of inherited retinopathies. *Prog. Retin. Eye Res.*, **43**, 108–128.
14. Kolstad, K.D., Dalkara, D., Guerin, K., Visel, M., Hoffmann, N., Schaffer, D.V. and Flannery, J.G. (2010) Changes in adeno-associated virus-mediated gene delivery in retinal degeneration. *Hum. Gene Ther.*, **21**, 571–578.
15. Park, T.K., Wu, Z., Kjellstrom, S., Zeng, Y., Bush, R.A., Sieving, P.A. and Colosi, P. (2009) Intravitreal delivery of AAV8 retinoschisin results in cell type-specific gene expression and retinal rescue in the Rs1-KO mouse. *Gene Ther.*, **16**, 916–926.
16. Vacca, O., Darche, M., Schaffer, D.V., Flannery, J.G., Sahel, J.A., Rendon, A. and Dalkara, D. (2014) AAV-mediated gene delivery in Dp71-null mouse model with compromised barriers. *Glia*, **62**, 468–476.
17. Petrs-Silva, H., Dinculescu, A., Li, Q., Min, S.H., Chiodo, V., Pang, J.J., Zhong, L., Zolotukhin, S., Srivastava, A., Lewin, A.S. *et al.* (2009) High-efficiency transduction of the mouse retina by tyrosine-mutant AAV serotype vectors. *Mol. Ther.*, **17**, 463–471.
18. Zhong, L., Li, B., Mah, C.S., Govindasamy, L., Agbandje-McKenna, M., Cooper, M., Herzog, R.W., Zolotukhin, I., Warrington, K.H. Jr, Weigel-Van Aken, K.A. *et al.* (2008) Next generation of adeno-associated virus 2 vectors: point mutations in tyrosines lead to high-efficiency transduction at lower doses. *Proc. Natl. Acad. Sci. USA*, **105**, 7827–7832.
19. Zhong, L., Zhao, W., Wu, J., Li, B., Zolotukhin, S., Govindasamy, L., Agbandje-McKenna, M. and Srivastava, A. (2007) A dual role of EGFR protein tyrosine kinase signaling in ubiquitination of AAV2 capsids and viral second-strand DNA synthesis. *Mol. Ther.*, **15**, 1323–1330.
20. Petrs-Silva, H., Dinculescu, A., Li, Q., Deng, W.T., Pang, J.J., Min, S.H., Chiodo, V., Neeley, A.W., Govindasamy, L., Bennett, A. *et al.* (2011) Novel properties of tyrosine-mutant AAV2 vectors in the mouse retina. *Mol. Ther.*, **19**, 293–301.
21. Zhong, L., Li, B., Jayandharan, G., Mah, C.S., Govindasamy, L., Agbandje-McKenna, M., Herzog, R.W., Weigel-Van Aken, K. A., Hobbs, J.A., Zolotukhin, S. *et al.* (2008) Tyrosine-phosphorylation of AAV2 vectors and its consequences on viral intracellular trafficking and transgene expression. *Virology*, **381**, 194–202.
22. Natkunarajah, M., Trittibach, P., McIntosh, J., Duran, Y., Barker, S.E., Smith, A.J., Nathwani, A.C. and Ali, R.R. (2008) Assessment of ocular transduction using single-stranded and self-complementary recombinant adeno-associated virus serotype 2/8. *Gene Ther.*, **15**, 463–467.
23. Stieger, K., Colle, M.A., Dubreil, L., Mendes-Madeira, A., Weber, M., Le Meur, G., Deschamps, J.Y., Provost, N., Nivard, D., Cherel, Y. *et al.* (2008) Subretinal delivery of recombinant AAV serotype 8 vector in dogs results in gene transfer to neurons in the brain. *Mol. Ther.*, **16**, 916–923.
24. Pang, J.J., Dai, X., Boye, S.E., Barone, I., Boye, S.L., Mao, S., Everhart, D., Dinculescu, A., Liu, L., Umino, Y. *et al.* (2011) Long-term retinal function and structure rescue using capsid mutant AAV8 vector in the rd10 mouse, a model of recessive retinitis pigmentosa. *Mol. Ther.*, **19**, 234–242.

25. Thapa, A., Morris, L., Xu, J., Ma, H., Michalakis, S., Biel, M. and Ding, X.Q. (2012) Endoplasmic reticulum stress-associated cone photoreceptor degeneration in cyclic nucleotide-gated channel deficiency. *J. Biol. Chem.*, **287**, 18018–18029.
26. Michalakis, S., Geiger, H., Haverkamp, S., Hofmann, F., Gerstner, A. and Biel, M. (2005) Impaired opsin targeting and cone photoreceptor migration in the retina of mice lacking the cyclic nucleotide-gated channel CNGA3. *Invest. Ophthalmol. Vis. Sci.*, **46**, 1516–1524.
27. Umino, Y., Solessio, E. and Barlow, R.B. (2008) Speed, spatial, and temporal tuning of rod and cone vision in mouse. *J. Neurosci.*, **28**, 189–198.
28. Kohl, S., Baumann, B., Broghammer, M., Jagle, H., Sieving, P., Kellner, U., Spegal, R., Anastasi, M., Zrenner, E., Sharpe, L.T. *et al.* (2000) Mutations in the CNGB3 gene encoding the beta-subunit of the cone photoreceptor cGMP-gated channel are responsible for achromatopsia (ACHM3) linked to chromosome 8q21. *Hum. Mol. Genet.*, **9**, 2107–2116.
29. Nishiguchi, K.M., Sandberg, M.A., Gorji, N., Berson, E.L. and Dryja, T.P. (2005) Cone cGMP-gated channel mutations and clinical findings in patients with achromatopsia, macular degeneration, and other hereditary cone diseases. *Hum. Mutat.*, **25**, 248–258.
30. Daniele, L.L., Lillo, C., Lyubarsky, A.L., Nikonov, S.S., Philp, N., Mears, A.J., Swaroop, A., Williams, D.S. and Pugh, E.N. Jr (2005) Cone-like morphological, molecular, and electrophysiological features of the photoreceptors of the Nrl knockout mouse. *Invest. Ophthalmol. Vis. Sci.*, **46**, 2156–2167.
31. Mears, A.J., Kondo, M., Swain, P.K., Takada, Y., Bush, R.A., Saunders, T.L., Sieving, P.A. and Swaroop, A. (2001) Nrl is required for rod photoreceptor development. *Nat. Genet.*, **29**, 447–452.
32. Roger, J.E., Ranganath, K., Zhao, L., Cojocaru, R.I., Brooks, M., Gotoh, N., Veleri, S., Hiriyanna, A., Rachel, R.A., Campos, M.M. *et al.* (2012) Preservation of cone photoreceptors after a rapid yet transient degeneration and remodeling in cone-only Nrl-/- mouse retina. *J. Neurosci.*, **32**, 528–541.
33. Matsumoto, B., Blanks, J.C. and Ryan, S.J. (1984) Topographic variations in the rabbit and primate internal limiting membrane. *Invest. Ophthalmol. Vis. Sci.*, **25**, 71–82.
34. Hendrickson, A.E. and Yuodelis, C. (1984) The morphological development of the human fovea. *Ophthalmology*, **91**, 603–612.
35. Yin, L., Greenberg, K., Hunter, J.J., Dalkara, D., Kolstad, K.D., Masella, B.D., Wolfe, R., Visel, M., Stone, D., Libby, R.T. *et al.* (2011) Intravitreal injection of AAV2 transduces macaque inner retina. *Invest. Ophthalmol. Vis. Sci.*, **52**, 2775–2783.
36. Aslanidi, G.V., Rivers, A.E., Ortiz, L., Song, L., Ling, C., Govindasamy, L., Van Vliet, K., Tan, M., Agbandje-McKenna, M. and Srivastava, A. (2013) Optimization of the capsid of recombinant adeno-associated virus 2 (AAV2) vectors: the final threshold? *PLoS ONE*, **8**, e59142.
37. Gabriel, N., Hareendran, S., Sen, D., Gadkari, R.A., Sudha, G., Selot, R., Hussain, M., Dhaksnamoorthy, R., Samuel, R., Srinivasan, N. *et al.* (2013) Bioengineering of AAV2 capsid at specific serine, threonine, or lysine residues improves its transduction efficiency in vitro and in vivo. *Hum. Gene Ther. Methods*, **24**, 80–93.
38. Kay, C.N., Ryals, R.C., Aslanidi, G.V., Min, S.H., Ruan, Q., Sun, J., Dyka, F.M., Kasuga, D., Ayala, A.E., Van Vliet, K. *et al.* (2013) Targeting photoreceptors via intravitreal delivery using novel, capsid-mutated AAV vectors. *PLoS ONE*, **8**, e62097.
39. Biel, M., Seeliger, M., Pfeifer, A., Kohler, K., Gerstner, A., Ludwig, A., Jaissle, G., Fauser, S., Zrenner, E. and Hofmann, F. (1999) Selective loss of cone function in mice lacking the cyclic nucleotide-gated channel CNG3. *Proc. Natl. Acad. Sci. USA*, **96**, 7553–7557.
40. Dyka, F.M., Boye, S.L., Ryals, R.C., Chiodo, V.A., Boye, S.E. and Hauswirth, W.W. (2014) Cone specific promoter for use in gene therapy of retinal degenerative diseases. *Adv. Exp. Med. Biol.*, **801**, 695–701.
41. Zolotukhin, S., Potter, M., Zolotukhin, I., Sakai, Y., Loiler, S., Fraites, T.J. Jr., Chiodo, V.A., Phillipsberg, T., Muzyczka, N., Hauswirth, W.W. *et al.* (2002) Production and purification of serotype 1, 2, and 5 recombinant adeno-associated viral vectors. *Methods*, **28**, 158–167.
42. Pang, J.J., Chang, B., Kumar, A., Nusinowitz, S., Noorwez, S.M., Li, J., Rani, A., Foster, T.C., Chiodo, V.A., Doyle, T. *et al.* (2006) Gene therapy restores vision-dependent behavior as well as retinal structure and function in a mouse model of RPE65 Leber congenital amaurosis. *Mol. Ther.*, **13**, 565–572.
43. Kong, F., Li, W., Li, X., Zheng, Q., Dai, X., Zhou, X., Boye, S.L., Hauswirth, W.W., Qu, J. and Pang, J.J. (2010) Self-complementary AAV5 vector facilitates quicker transgene expression in photoreceptor and retinal pigment epithelial cells of normal mouse. *Exp. Eye Res.*, **90**, 546–554.
44. Glushakova, L.G., Timmers, A.M., Pang, J., Teusner, J.T. and Hauswirth, W.W. (2006) Human blue-opsin promoter preferentially targets reporter gene expression to rat s-cone photoreceptors. *Invest. Ophthalmol. Vis. Sci.*, **47**, 3505–3513.
45. Boye, S.E., Boye, S.L., Pang, J., Ryals, R., Everhart, D., Umino, Y., Neeley, A.W., Besharse, J., Barlow, R. and Hauswirth, W.W. (2010) Functional and behavioral restoration of vision by gene therapy in the guanylate cyclase-1 (GC1) knockout mouse. *PLoS ONE*, **5**, e11306.
46. Pang, J.J., Boye, S.L., Kumar, A., Dinculescu, A., Deng, W., Li, J., Li, Q., Rani, A., Foster, T.C., Chang, B. *et al.* (2008) AAV-mediated gene therapy for retinal degeneration in the rd10 mouse containing a recessive PDEbeta mutation. *Invest. Ophthalmol. Vis. Sci.*, **49**, 4278–4283.